Brain Topogr (2016) 29:130–148
DOI 10.1007/s10548-015-0426-6

ORIGINAL PAPER

Spectral Signatures of Saccade Target Selection

Christine Carl · Joerg F. Hipp · Peter König · Andreas K. Engel

Received: 27 June 2014 / Accepted: 2 February 2015 / Published online: 18 February 2015

Abstract Action generation relies on a widely distributed network of brain areas. However, little is known about the spatiotemporal dynamics of neuronal activity in the network that gives rise to voluntary action in humans. Here, we used magnetoencephalography (MEG) and source analysis (n = 15, 7 female subjects) to investigate the spectral signatures of human cortical networks engaged in active and intrinsically motivated viewing behavior. We compared neuronal activity of externally cued saccades with saccades to freely chosen targets. For planning and execution of both saccade types, we found an increase in gamma band (~64–128 Hz) activity and a concurrent decrease in beta band (~12–32 Hz) activity in saccadic control areas, including the intraparietal sulcus and the frontal eye fields. Guided compared to voluntary actions were accompanied by stronger transient increases in the gamma and low frequency (<16 Hz) range immediately following the instructional cue. In contrast, action selection between competing alternatives was reflected by stronger sustained fronto-parietal gamma increases that occurred later in time and persisted until movement execution. This sustained enhancement for free target selection was accompanied by a spatially widespread reduction of lower frequency power (~8–45 Hz) in parietal and extrastriate areas. Our results suggest that neuronal population activity in the gamma frequency band in a distributed network of fronto-parietal areas reflects the intrinsically driven process of selection among competing behavioral alternatives.

Keywords Cortical saccade generation · Action selection · Gamma band activity · Intraparietal sulcus · Frontal eye fields · MEG

C. Carl · J. F. Hipp · P. König · A. K. Engel (✉)
Department of Neurophysiology and Pathophysiology, University Medical Center Hamburg-Eppendorf, Martinistrasse 52, 20246 Hamburg, Germany
e-mail: ak.engel@uke.de

C. Carl · P. König
Institute of Cognitive Science, University of Osnabrück, Albrechtstraße 28, 49069 Osnabrück, Germany

J. F. Hipp
Centre for Integrative Neuroscience, University of Tübingen, Paul-Ehrlich-Str. 17, 72076 Tübingen, Germany

J. F. Hipp
MEG-Center, University of Tübingen, 72076 Tübingen, Germany

Introduction

In everyday life we constantly face the challenge of selecting between several action alternatives. For example, a player in a soccer game acquiring the ball could either pass it on to a team member or take a shot at the goal. Also he has to re-adjust his choices both rapidly and flexibly to account for the continuous changes in player constellations resulting from his own movements and those of the others. Increasing evidence suggests that this form of action selection is not a sequential process where first the sensory input is acquired, followed by a decision and subsequent planning of an action. Rather, dynamic goal oriented behavior might be achieved by continuously encoding, updating, and weighting sensory evidence, action goals and plans for potential movements in parallel, so that different action alternatives are constantly at hand (Shadlen and Newsome 2001; Cisek and Kalaska 2010; Engel et al. 2013). These simultaneously evolving and competing action plans may form an integral part of a distributed and

emergent decision process that integrates perceptual, cognitive and motor functions (Cisek and Kalaska 2010). In support of this view, neural correlates of decision variables have been observed in various cortical and subcortical regions distributed across the brain, particularly including those structures that are specific for sensorimotor processing (Shadlen and Newsome 2001; Glimcher 2003; Cisek 2007; Cui and Andersen 2007; Gold and Shadlen 2007; Hoshi and Tanji 2007; Pesaran et al. 2008; Andersen and Cui 2009).

Physiological signatures of action selection have been studied extensively in non-human primates and implicate various areas of fronto-parietal sensorimotor association cortex in voluntary action selection in the presence of competing options (Haggard 2008; Kable and Glimcher 2009; Cisek and Kalaska 2010). These areas include effector specific regions in posterior parietal cortex and frontal premotor areas (Lawrence and Snyder 2006; Cui and Andersen 2007; Andersen and Cui 2009), which engage in oscillatory coupling during internally motivated choices (Pesaran et al. 2008). In humans, functional magnetic resonance imaging (fMRI), transcranial magnetic stimulation (TMS), or clinical lesion studies have provided evidence for distributed cortical substrates of action selection including parietal and premotor areas (Milea et al. 2007; Coulthard et al. 2008; Beudel and de Jong 2009; Oliveira et al. 2010; de Jong 2011; Hare et al. 2011). While investigations of perceptual decisions have emphasized the importance of oscillatory population activity mainly in the beta and gamma frequency range in such sensorimotor areas (Donner et al. 2009; Siegel et al. 2011; Gould et al. 2012; Wyart et al. 2012), the role of oscillatory dynamics in human voluntary action selection between competing behavioral alternatives remains largely unknown.

We here investigated oscillatory dynamics of voluntary action selection in the human brain. In particular, we used saccade target selection as a test case, which is a type of action selection where selection of sensory input and motor behavior are particularly tightly coupled. In order to address fast oscillatory dynamics of saccade selection in humans, we used MEG and source analysis, with a special focus on the cortical oculomotor network. Cortical areas of the human oculomotor network as known from various fMRI studies include frontal and supplementary eye fields, the parietal eye fields within the intraparietal sulcus, and dorsolateral prefrontal cortex (Sweeney et al. 2007; McDowell et al. 2008; Kagan et al. 2010; Anderson et al. 2012). Within this network, the parietal and frontal eye fields have been attributed to spatial aspects of orienting behavior and sensorimotor transformations from stimulus encoding to motor planning of the saccade (Medendorp et al. 2011). To study voluntary action selection we compared spectral signatures for selecting a saccade target among equally valuable targets with externally cued delayed saccades. While instructed saccades require only one action plan, free action selection among equal targets induces maximal competition between behavioral alternatives and may engage enhanced competition also at the neural level reflected in frequency specific power changes. Indeed, we could differentiate fast orienting responses for external saccade guidance from long lasting presumably competitive processes where a decision about an action emerges intrinsically, independent of any external instruction. More specifically, we found that oscillatory population activity of a fronto-parietal network within gamma and alpha—beta frequency range is associated with internally driven action selection between competing behavioral alternatives. This signature of neuronal activity within sensorimotor structures supports models suggesting that the selection of action emerges in a distributed way integrated with sensory and motor processes.

Materials and Methods

Participants

Fifteen healthy volunteers recruited mainly among university students participated in this study (seven female, eight male, mean age 25.7 ± 3.3). Participants received monetary compensation for their participation. All participants had normal or corrected-to-normal vision and had no history of neurological or psychiatric illness. According to self-report all subjects were right-handed.

Stimulation and Behavioral Task

Participants performed a delayed saccade task with saccades of two different amplitudes and 8 different directions (16 targets, Fig. 1). The delayed saccade task consisted of two experimental task conditions: In the memory-guided saccade condition, participants were asked to perform a guided saccade to one of the 16 targets indicated by a brief visual cue before the delay period. In the decision condition subjects could freely chose a saccade target out of the same 16 target positions (we will refer to these conditions as *guided* and *free* saccades, respectively).

At the beginning of each trial, subjects fixated for 800 ms a blue asterisk presented in the center of the screen. Surrounding the asterisk, 16 Gaussian patches were regularly arranged (width: 0.34°) on an inner and outer circle (distance from the asterisk: 5° and 10° respectively) serving as saccade targets. The background was grey, the peak of the Gaussian patches was white. Following fixation, the asterisk underwent a 200 ms isoluminant color change to either green (*free* saccade) or green with a red marker (*guided* saccade) that

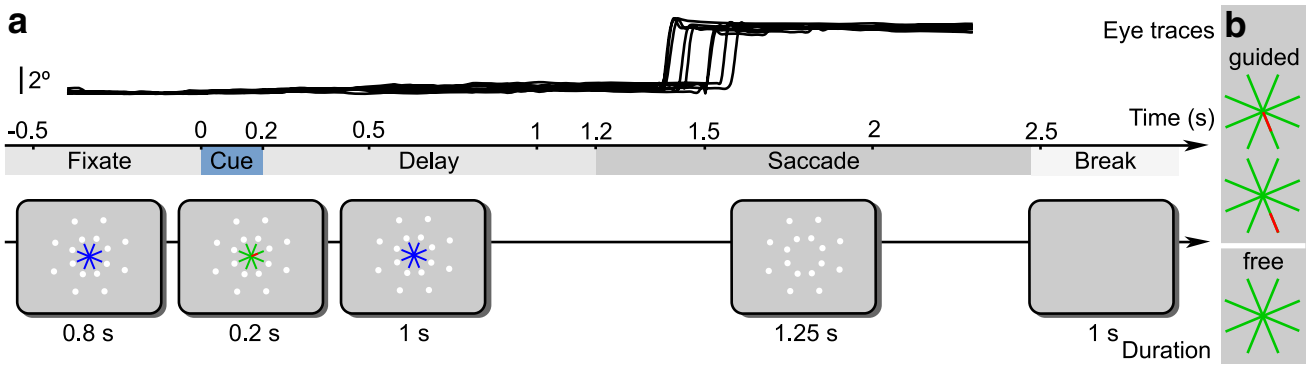

Fig. 1 Experimental task. **a** At trial onset subjects fixated a *blue asterisk* presented in the center of the screen. After a delay of 800 ms an isoluminant color change to *green* with a *red marker* instructed the target location of *guided* saccade trials. In half of the trials, a change to green without red marker instructed the subjects to freely choose one of the 16 targets. In the displayed example, the *red marker* instructed the subject to plan a short saccade to the right. After a delay of 1 s the *asterisk* disappeared and instructed the subject to execute the saccade. *Top* Representative eye traces of one participant over the first 9 trials for the displayed condition (*guided* short saccade to the upper right target). **b** Cue examples for *guided* and *free* saccade trials

indicated the task for each trial and served as a spatial cue. In the *guided* saccade condition the position of the red marker defined the direction of saccade target and instructed participants to prepare a saccade to this location. Moreover, the marker indicated a small saccade or a large saccade by being displayed at the inner or the outer part of the asterisk's branch, respectively. In the *free* decision task, a color change to a fully green asterisk instructed subjects to immediately choose one out of the 16 target alternatives and prepare a saccade to the freely chosen location. In both conditions participants had to maintain fixation during the following delay period of 1 s. Then, the asterisk disappeared instructing the subjects to perform the saccade. Subjects were told to maintain fixation at saccade target until it disappeared after 1.25 s. In between trials, a blank screen was presented for 1 s. In total each subject performed 702 trials (352 for *free* decision and *guided* saccade task, respectively; for the *guided* saccade task all 16 targets were cued equally often). Trials of all experimental conditions (*guided* and *free* saccades, as well as saccade targets in the *guided* saccade condition) were randomly presented. Each recoding was divided in two experimental blocks of approximately 33 min duration.

During the experiment, participants were seated in the MEG chamber. Stimuli were back-projected onto a screen at 60 cm distance with an LCD video projector (Sanyo Pro Xtrax PLC-XP51) and a two-mirror system. Stimuli were presented using the software Presentation (Neurobehavioral Systems, Albany, CA).

Analysis Software

All data analyses were performed in R (R Core Team 2013) and Matlab (MathWorks, Natick, MA) with custom implementations and the open source toolboxes Fieldtrip (Oostenveld et al. 2011), and SPM2 (http://www.fil.ion.ucl.ac.uk/spm/).

MEG Data Acquisition

We recorded MEG continuously with a 275-channel (axial gradiometer) whole-head system (Omega 2000, CTF Systems) in a magnetically shielded room. MEG data were digitized at 1200 Hz sampling rate (300 Hz low-pass filter). Off-line, we removed line-noise with notch-filters (at 50, 100, and 150 Hz), high- and low-pass filtered the data to 1 Hz and 170 Hz respectively (zero phase Butterworth IIR filter, filter order 4), and down-sampled it to 400 Hz.

Electrooculogram (EOG) Recordings

Along with the MEG, we recorded the EOG using the electroencephalography (EEG) channels of the CTF MEG system. Data were collected from AG/AGCL sintered flat electrodes (Easycap GmbH, Herrsching, Germany) with an analog passband of 0.16–300 Hz at a sampling rate of 1200 Hz. 7 EOG electrodes were placed over the nose, above and below each eye at the outer canthi, and below the left and right eye next to the nose. Data were referenced to an electrode placed at the tip of the nose during the recording. All electrode impedances were below 10 kΩ. Off-line, the EOG were high- and low-pass filtered (cut-off 1 and 170 Hz respectively, zero phase Butterworth IIR filter, filter order 4) and down-sampled to 400 Hz.

Structural MRI Acquisition

We acquired individual T1-weighted 1 mm^3 high-resolution structural images (MRIs) of each subject with a 3T Siemens MAGNETOM Trio Scanner using a coronal

magnetization-prepared rapid gradient echo sequence. These MRIs were used to construct individual head models for source analysis.

Eye Tracker Recording

Along with the neurophysiological data we recorded the eye position using an MEG compatible remote eye tracker system (iView X MEG 50 Hz, SMI, Berlin, Germany). The system monitored the right eye with an infrared camera to detect the pupil center and the corneal reflection of the infrared light source. After calibration (9 points) the system determined the gaze direction from the relative position of pupil and the corneal reflection at a rate of 50 Hz. Additionally, eye traces were digital to analog converted and fed to the MEG system on-line. This on-line procedure introduced temporal offsets on the order of 10th of milliseconds between eye tracker signal and MEG/EOG data and was characterized by undesirable ringing artifacts but served as a coarse reference for the first alignment of the eye tracker and MEG/EOG signals.

Off-line, we aligned the digital eye tracking data to the MEG/EOG in a 2-step procedure: First, we interpolated the 50 Hz signal to 400 Hz using cubic smoothing splines and computed the cross-correlation of the interpolated digital eye tracker signal with the analog version recorded with the MEG acquisition system. Then, we accounted for the offset identified by the latency of the peak in the cross-correlogram. In a second step, we refined the alignment and corrected for the offset between the EOG and the aligned eye tracker signal. To this end, we smoothed the data with a Savitzky-Golay filter (4th order, 102.5 ms), rectified and averaged all channels of both the EOG and the eye tracker signals, and estimated the offset from the peak of the cross-correlation.

To improve the range of validity of the eye tracker signal, we interpolated missing data. We detected periods with loss of eye tracking signal characterized by pupil size and gaze positions values close to zero. If these data segments were not identified as blinks (see "Artifact rejection" section), we interpolated the missing data by piecewise constant interpolation.

Artifact Rejection

Trials contaminated with muscle artifacts, signal jumps, or distortions of the magnetic field due to, for example, cars passing in front of the building were rejected off-line using semi-automated threshold procedures applied to the MEG signals. Since eye movements are part of the experimental design standard EOG based procedures to detect eye blinks fail. We detected eye blinks within each trial (−1.7 to 3.65 s from cue onset) by threshold-based procedures of the eye tracker and EOG signal in combination with visual inspection. For the eye tracker, data with vanishing pupil diameter coinciding with a small gaze parameter value for at least 60 ms were detected as potential blink artifacts. Blink detection within the EOG signal was based on a Fieldtrip function that detects high amplitudes in the z-transformed (across trials per condition) and band-passed (1–15 Hz) EOG data. If the sum of z-values divided by the square route of the number of channels exceeded 1 the period was marked as potential artifact. Trials were then rejected by visual inspection, if the actual trials of −0.4 s before to 2.3 s after the cue were contaminated by concurrent blink detection in the EOG and eye tracker data. Finally, we reviewed all MEG, eye tracker, and EOG signals to ensure good artifact rejection performance. On average across subjects, 17.0 ± 9.2 % (mean ± SD) of the trials were rejected.

Cleaning of Eye Movement Artifacts

Saccades induce two major kinds of eye movement artifacts: the corneo-retinal artifact, resulting from the rotation of the eyeball, and the saccadic spike artifact, which originates from the contraction of the extraocular muscles at saccade onset. Since we investigated MEG signals during the execution of regular saccades it is especially important to account for these artifacts. However, even during fixation periods eye movements occur in form of microsaccades and related artifacts can seriously distort the EEG or MEG signal (Yuval-Greenberg et al. 2008; Carl et al. 2012).

To clean the MEG signal from eye movement artifacts, while preserving all neuronal activity, we performed a two-step process. First, corneo-retinal artifacts were removed by linear regression based on the EOG signals. Second, we attenuated the saccadic spike artifact and possibly remaining eye movement related artifacts using independent component analysis (ICA). Note, that by applying these cleaning procedures throughout all analyzed data periods, we did not only suppress the artifacts originating from regular saccades but also those from microsaccades during fixation periods.

In order to remove corneo-retinal artifacts we used an EOG based linear regression technique (Gratton et al. 1983; Croft and Barry 2000; Schlögl et al. 2007). To obtain the appropriate subject-specific regression coefficients, we recorded 3 min of voluntary eye movements on a grey screen before and after each experimental block. In order to derive regression coefficients that capture the relation between EOG and MEG signals for all saccade directions, we instructed subjects to look actively around on the grey screen and confirmed good spatial coverage of viewing behavior by online visual inspection. The resulting

calibration signals were cleaned from non-saccadic artifacts, preprocessed, and then served to compute the linear relation between the EOG sensors (7 EOG electrodes referenced against an electrode at the nose, and reduced to 3 dimensions using principal component analysis) and each MEG channel (cf. Schlögl et al. 2007). MEG data were then cleaned by subtracting the weighted EOG signal.

EOG based regression without a radial component with posterior reference—although otherwise superior in performance to regressions based on such a component—performs weak in removing the saccadic spike artifact (cf. Plöchl et al. 2012). Because ICA has been shown to be especially suited to attenuate the saccadic spike artifact for EEG (Keren et al. 2010; Hassler et al. 2011; Kovach et al. 2011; Plöchl et al. 2012; Hipp and Siegel 2013), we subsequently applied ICA on the cleaned data (Hyvärinen and Oja 2000, Jung et al. 2000). ICA aims at finding a linear transformation of the sensor signal that separates the putative underlying sources by maximizing their statistical independence. Because the number of sources that can be separated by ICA is limited to the number of sensor channels, its performance for artifact suppression depends strongly on the data selection used for computation. To better isolate the saccadic spike artifact from the cerebral sources, it was proposed to augment it's contribution to the overall variance of the signal by restricting the signal to the dominant spectral range of the artifact (Kovach et al. 2011), selecting relevant data periods that emphasize the artifact but still include all cerebral sources of interest (Keren et al. 2010), or including additional 'virtual' channels that focus on the saccadic spike artifact (Hassler et al. 2011). A clear separation of eye movement artifacts from any other cortical signal related to the saccade is especially important when studying the cortical signals of saccade generation themselves. In the present study, we therefore maximized this separation by combining approaches of the above-cited EEG studies to our ICA analysis.

In detail, we computed a two-step ICA separately for each subject using the extended infomax algorithm (Lee et al. 1999). In order to remove saccadic spike artifacts, we computed an ICA on the band limited data of 24–160 Hz, a spectral band that includes the characteristic spectral range of the saccadic spike artifact (Jerbi et al. 2009; Keren et al. 2010; Kovach et al. 2011; Carl et al. 2012). The ICA was computed for each subject on the concatenated data of the trial periods and additional perisaccadic time intervals of each trial (50 ms before and after the saccade onset). Artifact components were selected based on visual inspection of their topography, the spectral power and the single trial saccade related response of the independent components (cf. Carl et al. 2012, for a spatial distribution of the saccadic spike artifact in MEG). To further reduce cardiac artifact components and possibly remaining eye movement artifacts we rerun the ICA analysis on the broadband cleaned signal including EOG channels normalized to the standard deviation of the MEG channels. With this 2-step approach, we found on average one saccadic spike component per subject and 1–2 other artifactual components.

Note that we performed all comparisons of experimental conditions in source space, thereby further reducing the risk of artifactual contamination by saccade related artifacts (cf. Hipp and Siegel 2013).

Behavioral Analysis

For detection of regular saccades we employed a velocity threshold based algorithm on the eye tracker data. If coupled with a minimum saccade duration criterion, this algorithm has very few parameters and is accurate in the face of stereotypical eye movements such as those analyzed here (Salvucci and Goldberg 2000). Because the optimal velocity threshold parameter depends on preprocessing and sampling of the recorded data, as well as on saccade amplitudes, we defined the velocity threshold in a data-driven approach. We adapted the thresholds manually for the saccade amplitudes in our task (5° and 10°) so that saccades were detected while the number of false positives was minimized. We achieved this by visual inspection of the data, taking into account a priori knowledge on saccade timing. We defined periods as regular saccades in which the eye movement velocity was higher than 26.9°/s for a duration of at least 22.5 ms. Periods where the saccade velocity exceeded 67.1°/s were defined as saccades irrespective of saccade duration. We combined all saccade intervals that were less than 7.5 ms apart from each other into a single saccade interval. All other periods were labeled as fixations.

We aligned all trials either to the cue or to saccade onset. Precise alignment to saccade onset relied on the EOG signal with higher temporal resolution than the eye tracker signal.

The behavioral analysis revealed that subjects showed a considerable variability in saccade onset and also initiated saccades before the 'go' signal. To maximize the number of trials for analysis and at the same time ensure sufficient data length of the saccade planning and re-fixation period, we accepted trials with saccades that were performed within a broad time window from 250 ms before to 450 ms after the 'go' signal. In a next step, we rejected all trials with incorrect saccade orientation or amplitude. For saccade categorization we applied drift correction at the fixation period before the cue onset (−300 to −100 ms) and ensured that the subjects fixated the asterisk before saccade onset within a tolerance angle of 2.5°. In the *guided* saccade condition saccade target was considered correct if the closest location was the cued

one, for *free* decision trials chosen saccade target was defined as the closest of the 16 target points if it was maximally 2.5° away from it. Overall we discarded 15.8 ± 9.2 % (mean ± SD) of the trials because of faulty behavioral performance.

For the decision contrast we modified the definition of valid trials. Neuronal signatures of free target selection can occur within the whole delay period. Consequently, for all decision related contrasts (*free* vs. *guided* saccades, *free* or *guided* saccades vs. baseline respectively) we analyzed the entire delay period of 1.2 s. For these analyses, we rejected all premature saccades that were performed before the 'go' signal. For 2 out of the 15 subjects less than 25 % of the trials remained after rejecting these premature saccades. We excluded these two subjects in the analyses of decision processes.

To test for significant differences between *free* and *guided* saccades in saccade metrics like saccade latency, velocity, duration, or accuracy, we performed random permutation tests: For each saccade metric of interest (or the variance thereof), we computed the mean difference between *free* and *guided* trials, averaged across subjects and compared this value to the null hypothesis distribution generated by randomly permuting *free* and *guided* condition labels within each subject and computing the same difference for 10,000 iterations.

If subjects systematically preferred left or right target sides in the free decision condition, this may have led to systematic power changes due to lateralized power changes related to saccade preparation confounding decision related contrasts. To test if subjects had a preference in selecting specific saccade targets in the free decision condition we tested for such a bias within subjects and across subjects in an analysis that mirrored the fixed effects analysis of conditional spectral power differences. In both cases, we encoded chosen saccade targets as 8 directional vectors of unit length from the initial fixation position at the screen center to the direction of the Gaussian blobs. We then computed the average direction vector across trials within each subject. If all saccade target directions are chosen equally often this vector results in zero. In the single subject analysis we tested if the average direction vector for chosen targets in the *free* saccade condition was significantly different from a distribution of average vectors generated by 10,000 times drawing from a uniform distribution of saccade target directions. Equivalent to the statistical comparisons of spectral power between *free* and *guided* trials we also tested for a significant difference in target distribution of the trials between *free* and *guided* saccades across subjects: We computed the mean difference of the average saccade direction vector for *free* and *guided* saccades (*free-guided*) across subjects and compared this difference to a random permutation distribution. This distribution was generated by 10,000 times permuting condition labels of *free* and *guided* saccades within each subject, computing the difference in average direction between these conditions and calculating the average of these values across subjects.

Free target selection might further be influenced by the history of previous saccade targets. In order to evaluate whether the saccade target of the previous trial influenced the choice of the next trial, we calculated the frequency of *free* decision trials with the same saccade target as the preceding trial, irrespective of whether this trial was a *free* or *guided* saccade. We tested whether the frequency of choosing the same saccade target was significantly different from a binomial distribution with the probability of choosing the same target $p = 1/16$ within each subject.

Spectral Analysis

We estimated spectral power using the multi-taper method based on discrete prolate spheroidal (slepian) sequences (Thomson 1982; Mitra and Pesaran 1999). Spectral estimates were computed across 19 logarithmically scaled equidistant frequencies from 5.7 to 128 Hz (in 0.25 octave steps) and up to 34 points in time from −1.25 to 0.4 s for the saccade-aligned data (−0.05 to 1.6 s for the cue-aligned data, 0.05 s steps). We adjusted the temporal and spectral smoothing using the multi-taper method so that it matched approximately 250 ms and 3/4 octaves, respectively. For frequencies ≥16 Hz we used temporal windows of 250 ms and adjusted the number of slepian tapers accordingly to the spectral smoothing of 3/4 octaves. For frequencies <16 Hz we adjusted the time window to yield a frequency smoothing of 3/4 octaves with a single taper. To estimate signal power, we multiplied the complex spectrum with its complex conjugate and averaged this across trials and tapers. We characterized the power response relative to the pre-stimulus baseline.

To derive the baseline power estimate, we selected analysis windows that stopped at the onset of the instruction cue, where possible (for frequencies >10 Hz). For frequencies ≥16 this resulted in a baseline at $t = -0.125$ s. Owned to the size of the analysis window for low frequencies, and given that valid data started −400 ms before the presentation of the instruction cue, the baseline reached into the presentation of the instruction cue for frequencies ≤9.5 Hz (9.5 Hz: 0.015 s, 8 Hz: 0.093 s, 6.7 Hz: 0.185 s, 5.6 Hz: 0.298 s).

Source Analysis

Estimating the neural activity at the source level requires a physical forward model or leadfield that describes the electromagnetic relations between sources and sensors. To derive this physical relation we employed a single-shell

volume conductor model (Nolte 2003). We computed two physical forward models for each subject that differed in spatial resolution and distribution of source locations. Sources of one model covered the whole brain with a regular grid in MNI space of 1 cm resolution resulting in 3648 sources. Sources of the second model were distributed with a spacing of 1 cm on a shell lying 1 cm beneath the skull (for a detailed description of the source grid see Hipp et al. 2011). This model comprises only 400 source locations and samples the source space more sparsely than the first model. However, the second model still ensures homogeneous coverage across the cortex. To derive the individual physical forward models for each subject, we affine transformed source locations into individual head space using the participants' individual T1-weighted structural MRI and aligned the MEG sensors to the head geometry based on 3 fiducial points (nasion, left and right ear, defined in the MEG by 3 head localization coils).

We used adaptive linear spatial filtering ('beamforming' Van Veen et al. 1997; Gross et al. 2001) to estimate the amplitude of neural population signals at cortical source level. In short, for each source location, three orthogonal linear filters (for the three orientations at each source) were computed that pass activity from that location with unit gain, while maximally suppressing activity from any other source. Subsequently, the filters were linearly combined to a single filter that points to the direction of the dominant dipole. For each experimental contrast (e.g., activation versus baseline or left versus right saccades), we derived a separate filter estimation from the real part of the cross-spectral-density matrix at each point in time and frequency. To avoid a bias of the filter, we randomly choose trials to equalize the trial number between the experimental contrasts at hand before computing the filter. To derive the complex source estimates, the complex frequency domain data were then multiplied with the real-valued filter. To estimate power in source space we multiplied the complex spectral estimate with its conjugate and averaged across all trials and tapers.

For illustration of the sources we overlaid the functional data onto the structural MRIs of the segmented surface or cut surface of the 'colin27' MRI T1 average (Holmes et al. 1998), masked non-significant values (see "Statistical analysis of spectral power" section), and interpolated the source data to 1 mm resolution. We express changes of spectral power either as percentage change (relative to baseline), as contrast, or as z-scores (cf. Medendorp et al. 2007).

Definition of Regions of Interest

To further investigate neuronal activity in areas of the cortical oculomotor network (Sweeney et al. 2007; McDowell et al. 2008; Anderson et al. 2012), we defined regions of interest (ROIs) based on coordinates of areas identified in an fMRI study that examined cortical areas involved in saccade planning and execution in a similar delayed saccade task (Kagan et al. 2010). We adapted the selection and labeling of ROIs to better suit the spatially coarser resolution of MEG. We defined 3 regions along the intraparietal sulcus: the posterior intraparietal sulcus (pIPS; V7 in Kagan et al. 2010), middle intraparietal sulcus (mIPS; union of areas IPS2 and retIPS in Kagan et al. 2010), and anterior intraparietal sulcus (aIPS). The ROI for the frontal eye fields (FEF) was defined as the union of lateral and medial frontal eye fields (cf. Kagan et al. 2010). We further defined a ROI for the supplementary eye fields (SEF) and the dorsolateral prefrontal cortex (dLPFC). Furthermore, we created a ROI for early visual areas (V1).

For defining the frontal and parietal ROIs we transformed Talairach coordinates of ROI centers reported in Kagan et al. (2010) into MNI space using the transform functions suggested by Lancaster et al. (2007) and identified nearest neighbors of this MNI coordinate to the source location of the used leadfield (1 nearest neighbor for the single shell leadfield and 7 nearest neighbors for the fine grained leadfield covering the whole cortex). The position of V1 was defined as all nearest neighbors of the source locations of the used leadfield to the template of Brodman area 17 provided by MRIcroN. Using this ROI definition for the template brain, employed ROI labels may not denote exact anatomical regions within the single subjects. However, it should be noted that source analysis of MEG data is an ill-posed problem and results at best in a spatially blurred image of the true brain activity. We therefore defined ROIs considering these limits in spatial resolution of the MEG.

Statistical Analysis of Spectral Power

For statistical testing of differences in spectral power between conditions, we first log-transformed the power values to render the distributions more normal. For each subject, we then computed a 2-sided paired t test of spectral power between conditions for each source or ROI at each time and frequency window, transformed t-values into z-scores, averaged across subjects, and multiplied with the square root of the number of subjects. This procedure implements fixed-effects statistics for each time–frequency-voxel volume, a test of the typicality of an effect within a relatively homogeneous subset of the population.

We made little a priori assumptions and tested for spectral power effects throughout the cortex and resolved in time and frequency. More specifically, we investigated power differences at 5 continuous frequency ranges corresponding approximately to the classical frequency bands

known from EEG and MEG (theta 5.7–8 Hz, alpha 8–16 Hz, beta 16–32 Hz, low gamma 32–64 Hz, and high gamma 64–128 Hz) and time intervals of 100 ms length in 100 ms steps if not indicated otherwise. The high dimensional time–frequency-voxel space results in substantial multiple comparisons that need to be accounted for. We differentiated two cases in our analysis, strong baseline effects and more subtle condition contrasts:

Since the comparison of activation against baseline generally yields strong effects, we computed these power differences on the more detailed regular source grid covering the whole cortex (3648 sources) and accounted for multiple comparisons across the time–frequency-voxel space using false discovery rate (FDR) correction (Benjamini and Hochberg 1995; Genovese et al. 2002) with $q = 0.05$.

For comparing the smaller signal differences between *free* versus *guided* saccades or between horizontal saccade directions we employed the forward model that covers the cortex in a single shell at 1 cm below the skull's surface comprising 400 sources or an adapted subset thereof. We accounted for multiple comparison correction within this 4 dimensional time–frequency-voxel space (2 dimensions for space because of the planar geometry of the source grid) by a cluster based random permutation approach. In particular, we identified bins in the time–frequency-voxel space whose t-statistic exceeded a threshold corresponding to a significance level of $p < 0.05$, resulting in a binary matrix with values of 1 for bins larger than the threshold. For each time and frequency bin separately, we identified clusters in voxels of this binary matrix that are linked through direct neighborhood relations (neighboring voxels with 1). Such a cluster corresponds to a network of cortical regions with different spectral power between conditions that is continuous across space. For each cluster, we defined its size as the integral of the statistical z-scores of the power differences between conditions across the volume of the cluster and tested its statistical significance using a random permutation statistic: For each separate time and frequency bin, we repeated the cluster identification 1000 times (starting with the t-statistic between conditions) with shuffled condition labels to create an empirical distribution of cluster sizes under the null-hypothesis of no difference between conditions. The null-distribution was constructed from the largest clusters (two-tailed) of each resample across all time and frequency bins, therefore accounting for multiple comparisons across space, time, and frequency bins (Nichols and Holmes 2002).

Note that, direction specific neuronal activity for saccades to the left and the right can be assumed to be largely mirror symmetric and hemispherically lateralized (cf. Medendorp et al. 2007; Van Der Werf et al. 2008). Therefore, we combined data for the direction specific contrast by subtracting power of right from left homologous source locations and dividing this by 2. Data was then visualized only on the left hemisphere.

To further elucidate the spectro-temporal evolution of signal power at a finer scale, we show time frequency spectra at selected ROIs across all time frequency points computed in the source analysis (see "Spectral analysis" section). In order to visualize the extent of important spectral changes in frequency bands and latencies, we mask spectra statistically, using an uncorrected threshold at a significance level of $p < 0.05$. Direction specific neuronal activity for saccades to the left and the right can be assumed to be largely mirror symmetric and lateralized to the contralateral hemisphere. Therefore, we combined data for the direction specific contrast by subtracting power of right from left homologous ROIs and dividing this by 2. In order to illustrate the directional specificity for *free* and *guided* saccades separately, we computed the Michelson contrast: We subtracted average of left from average of right saccades divided by the mean sum of the power of both conditions and subsequently averaged mirrored left and right ROIs. For all other investigations, where lateralization of direction independent saccade related activity was weak, we averaged spectral power of homologous ROIs of the two hemispheres.

Results

We investigated neuronal activity related to human saccade target selection, planning, and execution by measuring MEG and gaze position in a delayed saccade task (Fig. 1) using a fixed-effects analysis (15 subjects, mean age 25.7 ± 3.3, for decision related contrasts 2 subjects out of these 15 were excluded). In each experimental trial, subjects either performed a cued saccade to one of 16 targets or were free to choose a target. We first studied general signatures of saccade planning and execution. Then, by contrasting *free* and *guided* saccades we differentiated voluntary action selection processes between competing alternatives from guided saccade selection.

Oscillatory Signatures During Saccade Planning and Execution

We pooled data of *guided* and *free* saccades across all directions and amplitudes, to investigate changes in local population activity relative to a pre-cue baseline reflecting processes of saccade planning and execution. In particular, we analyzed changes in spectral power of saccade-aligned signals in 6 time windows ranging from 600 ms before to 400 ms after saccade onset and in 5 frequency bands from

the theta (5.7–8 Hz) to the high gamma range (64–128 Hz) (Fig. 2).

We found sustained and spatially widespread changes in spectral power during saccade planning and execution in fronto-parietal areas (t test, $p < 0.05$, FDR corrected for number of sources, time, and frequency windows, $n = 3648 \times 6 \times 5$, maximal absolute percentage change of significant voxels across time and space: theta: 74.89 %; alpha: 50.90 %; beta: 69.74 %; low gamma: 28.68 %; high gamma: 15.01 %). During the delay period, before saccade execution, we identified a sustained increase in high gamma power (64–128 Hz) in posterior and medial parietal areas along the intraparietal sulcus and precuneus. This activity extended to anterior regions of intraparietal sulcus and to the frontal and supplementary eye fields before the upcoming saccade. Following the saccade, gamma power further increased in posterior and medial parietal areas. In the beta frequency range (16–32 Hz), spectral power was reduced along the intraparietal sulcus in the superior parietal lobe during the delay period. Shortly before saccade execution the decrease in beta power extended to frontal regions around the frontal eye fields and the supramarginal gyrus, where it persisted during re-fixation. After saccade execution, also power in the alpha frequency band (8–16 Hz window) reduced in posterior portions of the parietal and occipital cortex. After saccade onset a transient broadband spectral power increase (all frequency windows up to 64 Hz) originated from early visual areas. The medial portion of extrastriate visual areas also showed a sustained increase in alpha power during the delay period.

To resolve the time-courses and bandwidth of the observed spectral power changes, we computed time–frequency spectrograms with a high resolution for selected ROIs of the fronto-parietal saccade related network (see "Materials and Methods" section, Fig. 3). Increases in the gamma band in the fronto-parietal regions (FEF, aIPS, mIPS, and pIPS) were sustained throughout the delay period (from time $t = -600$ to 0 ms) and ranged from 45 to 128 Hz. Increases intensified at saccade onset in all these ROIs and persisted in parietal ROIs and early visual areas (V1) during the whole re-fixation period that was analyzed (up to 400 ms after saccade onset). The decrease in beta power, strongest at 16–23 Hz, was sustained in frontal and parietal ROIs (FEF, aIPS and mIPS) throughout the analysis window (starting 600 ms before saccade onset) and appeared in SEF approximately 300 ms before the saccade. A sustained alpha increase throughout the delay was strongest in posterior areas (pIPS, V1). pIPS and V1 also showed strong spectral changes during re-fixation: The transient broadband increase around 32 Hz at approximately 100 ms after saccade onset was followed 50 ms later by a decrease in intermediate frequency range at 8–23 Hz. Power in the low frequency range of theta below 8 Hz was increased and probably reflected visual evoked event related responses.

In summary, these results revealed a dichotomy of oscillatory activity in widespread fronto-parietal networks

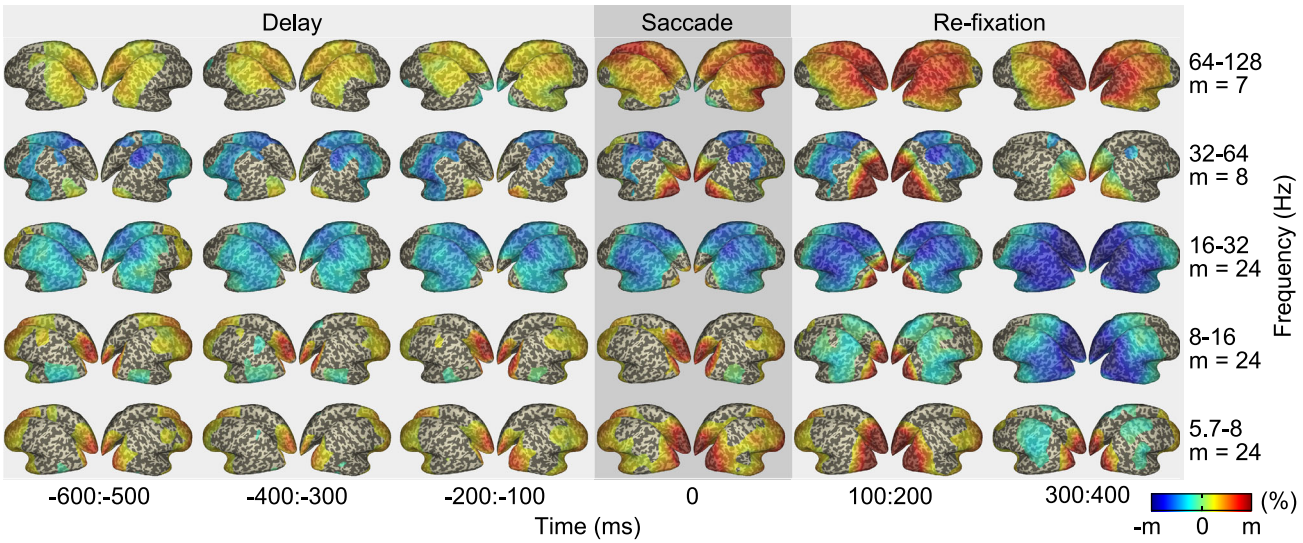

Fig. 2 Spectral power changes during saccade planning and execution. Average change in spectral power relative to pre-cue baseline (~52–125 ms before cue onset, depending on the frequency) across *free* and *guided* saccades. Average power changes are shown for different points in time and frequency resolved in cortical space. Data are aligned to saccade onset (at time t = 0 ms). The *color bar* limits are adapted to the specific range of power changes for each frequency (denoted by *m*, e.g. for the beta band the color map shows relative frequency changes compared to baseline from −24 to +24 %). Power changes are statistically masked for significant difference from zero (t test, $p < 0.05$, FDR corrected)

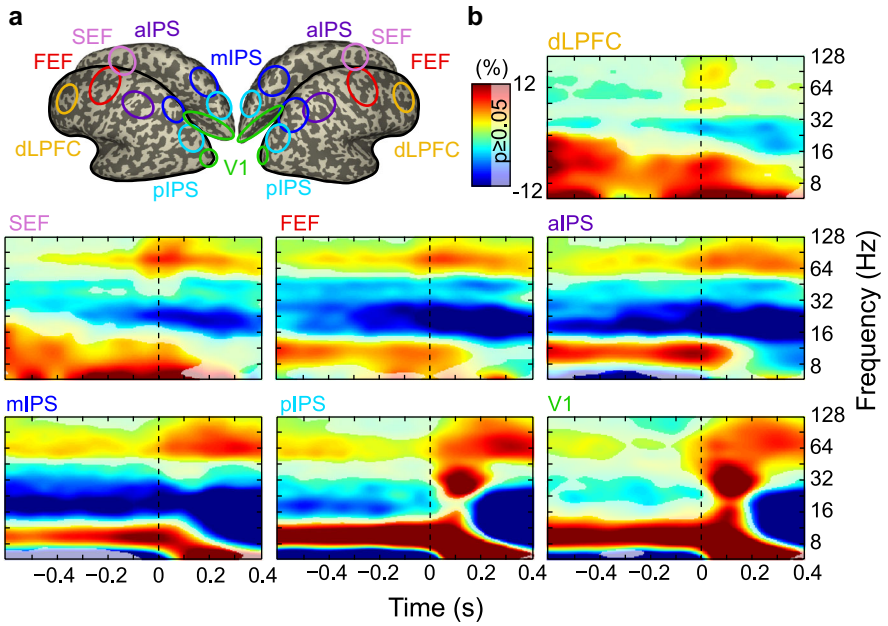

Fig. 3 Spectral power changes during saccade planning and execution in selected ROIs. **a** *Encircled areas* indicate the spatial location of each ROI on the inflated template brain (*dLPFC* dorsal lateral prefrontal cortex, *SEF* putative human homologue of supplementary eye field, *FEF* putative human homologue of lateral and medial frontal eye field, *aIPS*, *mIPS*, *pIPS* anterior, medial and posterior intraparietal sulcus, *V1* early visual cortex). **b** Relative spectral power changes of saccade-aligned data (saccade onset at time t = 0 ms, *dotted line*) for the ROIs relative to baseline (~52–125 ms before cue onset, depending on the frequency). Data are pooled across homologous areas in the two hemispheres. *Unmasked regions* denote significant difference from zero (*t* test, $p < 0.05$, uncorrected for multiple comparisons)

associated with delayed saccades, with increases of high frequency (gamma) activity and decreases of low frequency (beta) activity. Furthermore, visual areas were characterized by strong broadband power changes after the saccade.

Oscillatory Signatures of Saccade Target Selection

Next, we investigated oscillatory activity specifically related to the selection of saccade targets. To this end, we contrasted spectral power between *free* and *guided* saccade trials. The reasoning was that, in *guided* trials, the spatial cue immediately leads to the selection of a specific motor plan while in *free* saccade trials subjects were required to choose between 16 possible targets. Consequently, early cue-related activity should capture the instructed selection of a specific motor action in *guided* trials, while we expected a prolonged signature of the action selection process for *free* trials.

Therefore, we analyzed power differences between *free* and *guided* trials for cue (Fig. 4b) as well as saccade-aligned data (Fig. 4c) across the whole delay phase in 10 time windows starting 50 ms before cue onset until 400 ms after the go signal for the cue-aligned data (time windows for saccade-aligned data were chosen equivalently).

In response to the cue, we found more gamma (64–128 Hz) and theta power (5.7–8 Hz) in occipital and posterior parietal cortex for *guided* compared to *free* saccade trials (cluster based random permutation test, $p < 0.05$, corrected for multiple comparisons of number of sources, time, and frequency windows, $n = 400 \times 10 \times 5$, 20.97 % (theta) and 6.61 % (gamma) maximal reduction of free compared to guided saccades, Fig. 4b). In the delay phase before saccade initiation until re-fixation (from 600 ms before to 200 ms after saccade onset) high gamma power was stronger in a fronto-parietal network when freely choosing saccade targets compared to *guided* saccade trials (cluster based random permutation test, $p < 0.05$, corrected for multiple comparisons of number of sources, time, and frequency windows, $n = 400 \times 10 \times 5$, Fig. 4c, 4.87 % maximal increase). This network comprised frontal and supplementary eye fields as well as parietal areas around precuneus and along the intraparietal sulcus from its anterior-medial to posterior parts. For lower frequencies in the alpha and beta frequency range (8–16 Hz and 16–32 Hz) we found a significant reduction of power during the delay period in widespread regions of posterior parietal cortex for *free* saccades compared to *guided* saccades. During execution and re-fixation this reduction was strongest at infero-temporal areas (16.42 %

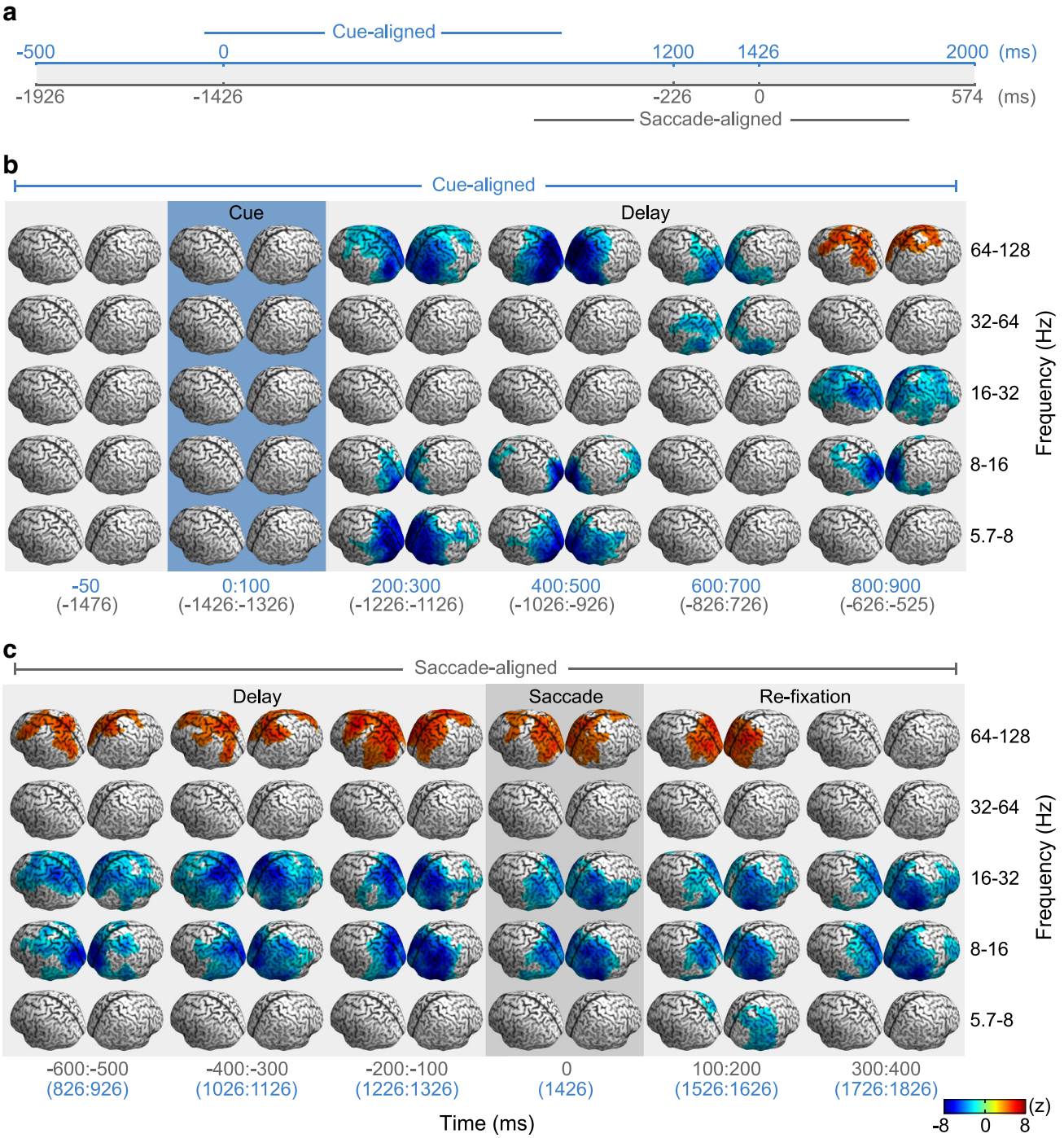

Fig. 4 Saccade target selection. Spatio-temporal evolution of differences in spectral power between *free* and *guided* saccades (*free-guided*). Differences from zero were statistically assessed for the time period from cue presentation until re-fixation by cluster based random permutation correcting for multiple comparisons of number of voxels, time windows, and frequency windows ($p < 0.05$, we show a relevant subset of comparisons). Functional maps are masked by the extent of the identified clusters and are illustrated on a 3D cortical surface. **a** Time windows chosen for the analyses shown in B and C are partly overlapping. **b** Response to cue is shown with cue-aligned data. Time points with respect to cue are depicted in *blue*, equivalent timing for saccade alignment with respect to the mean saccade latency at 226 ms after the go cue is shown below in *brackets*. **c** Activity during delay and subsequent saccade is shown in alignment to saccade onset. Time points with respect to saccade onset are depicted in *grey*, equivalent timing for cue alignment considering mean saccade latency is shown in *blue*

(alpha) and 13.34 % (beta) maximal reduction of *free* compared to *guided* saccades).

To understand the origin of the differences between *free* and *guided* saccades we analyzed power changes relative to pre-cue baseline separately for both conditions at several locations within the fronto-parietal network (Fig. 5). The analysis revealed that the difference in gamma power in the fronto-parietal network during the delay interval before saccade onset (starting approximately 600 ms before saccade onset) was caused by a gamma power increase in *free* saccade trials relative to baseline rather than a power decrease in *guided* saccade trials. The reductions in alpha and beta power relative to pre-cue baseline appeared to result from a stronger decrease in beta power in the *free* saccade compared to the *guided* saccade condition and a stronger increase in alpha power in the *guided* saccade condition.

Behavioral Analysis of Saccade Metrics

These findings suggest sustained increased gamma power accompanied by reduced alpha to beta power in a fronto-parietal network during the delay reflecting the selection between different possible motor plans in *free* saccade trials. A potential confound of the observed effects may be systematic differences in saccade statistics between *free* and *guided* saccades that might induce the observed power differences between conditions. To test for this possible confound, we compared chosen target frequencies and saccade metrics between conditions.

In a subject specific analysis six out of the 13 subjects showed a significant bias in choosing specific saccade targets more frequently than others in the *free* decision trials. However, a random permutation test of the average direction difference of saccade targets across subjects between *free* and *guided* condition (see Materials and Methods section), which mirrored the statistical analyses in spectral power differences between free and guided saccades, did not show a significant condition specific preference of saccade target direction ($p = 0.3902$). This suggests that the observed selection specific differences in power are not a mere reflection of saccade metrics but reflect differences in the neuronal processes related to action selection.

We further characterized saccade metrics and their condition specific differences. Across conditions saccades lasted on average 61.70 ± 29.01 ms (mean ± SD), and had a velocity of 230.59 ± 97.53°/s (mean ± SD). Saccades occurred on average 225.81 ± 72.67 ms (mean ± SD) after the *go* cue presentation. Mean accuracy of saccade target was 1.04 ± 2.10 ° (mean ± SD, distance of fixation after saccade from the center of the Gaussian blobs).

We found that average saccade latencies of *free* selection trials were 5.31 ms larger than those of *guided* saccades ($p = 0.0058$, random permutation test) and showed slightly higher variance (difference between *free* and *guided* latency variance: 0.52 ms, $p = 0.02$, random permutation test). Although significant, these differences between conditions are negligible with respect to the spectral power comparison since they cover only ∼2 % (∼0.2 % for the difference in variance) of even the shortest analysis window for the frequency transform. While saccade accuracy and duration did not differ significantly between conditions (mean accuracy difference = −0.0005°,

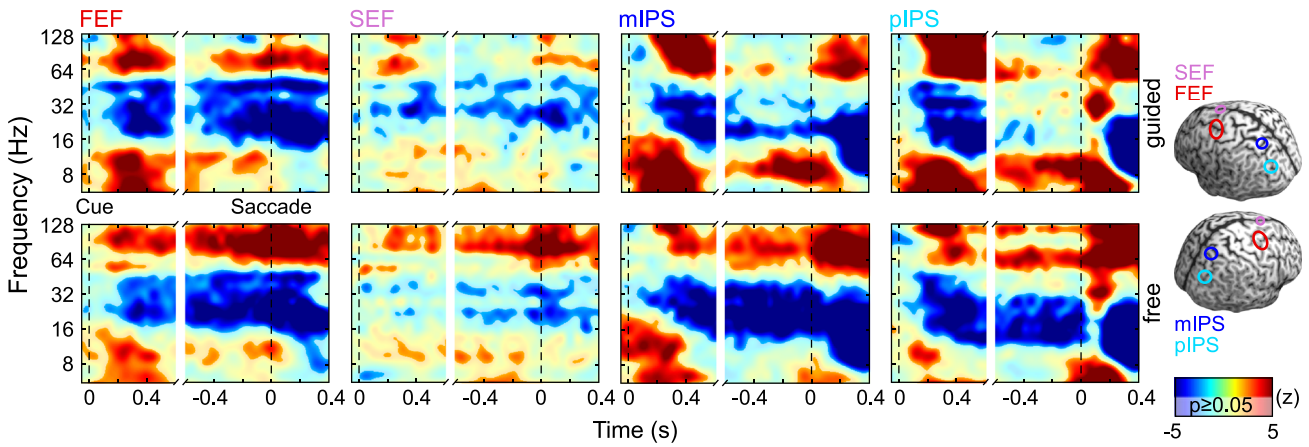

Fig. 5 Spectral power changes for *free* and *guided* saccades in fronto-parietal ROIs. Power changes relative to baseline (∼52–125 ms before cue onset, depending on the frequency) of *guided* (*upper row*) and *free* (*lower row*) saccades during saccade planning, saccade execution, and re-fixation in FEF, SEF, mIPS and pIPS averaged over both hemispheres. Data are aligned to cue onset (t = 0 ms, *dotted line*) for the *left part* of the spectrogram and to saccade onset (t = 0 ms, *dotted line*) for the *right part* of the spectrogram. Power changes are represented as statistical z-values, unmasked regions show significant differences from zero (*t* test, $p < 0.05$, uncorrected for multiple comparisons)

$p = 0.5117$, mean duration difference $= -0.56$ ms, $p = 0.6989$, both random permutation test), free saccades were on average 8.82°/s faster than guided saccades ($p = 0.0047$, random permutation test).

Evaluation of whether subjects employed a specific behavioral strategy for target selection revealed that 10 out of 13 subjects showed a significant inhibition in performing the saccade to the same target as in the previous trial (binomial test within each subject, $p < 0.05$).

Encoding of Saccade Direction

In the above analysis, we pooled the data for saccades to different spatial locations. This identifies processes involved in selection, planning, and execution of saccades independent of the saccade metrics. Despite its limited spatial resolution, hemispheric specificity to the left and right visual hemifields is accessible with MEG. In order to study neuronal processes encoding saccade metrics, we exploited this property and compared the difference in neuronal activity between the left and right hemispheres for trials with left- and rightward saccades closest to the horizontal midline of the monitor. More specifically, we pooled *free* and *guided* saccades and analyzed spectral power of the difference of left- from rightwards saccades. By averaging hemispheres through mirroring homologous sources across the midline (cf. "Statistical analysis of spectral power" section) we compared spectral power contralateral and ipsilateral to saccade direction. We restricted the analysis to fronto-parietal and visual sources that we found to be related to saccade preparation (Fig. 6a, cf. Fig. 2) and to 3 time windows. These time windows separated the delay phase from 600 to 100 ms before saccade onset from the saccade execution at time $t = 0$ ms and re-fixation from 100 to 400 ms after saccade onset. We employed cluster based random permutation tests ($p < 0.05$, corrected for multiple comparisons of number of sources, time, and frequency windows, $n = 95 \times 3 \times 5$, Fig. 6a).

During preparation of saccades, we found significantly stronger power in the low gamma frequency range (32–64 Hz window) for sites in pIPS contralateral to saccade direction. During re-fixation low gamma power was stronger contralateral to saccade direction at extrastriate regions around the junctions of lateral occipital sulcus and inferior temporal sulcus and around pIPS. During saccade execution we did not find significant lateralization effects in the gamma range. Power in all lower frequency windows (theta 5.7–8 Hz, alpha 8–16 Hz, beta 16–31 Hz) was significantly lower for sites contralateral than for sites ipsilateral to saccade direction during delay, execution, and re-fixation at extended regions of the posterior cortex. This difference was largest in the alpha range around pIPS during delay and at extrastriate areas at the junctions of lateral occipital sulcus and inferior temporal sulcus during re-fixation.

To resolve the time-courses and bandwidth of the observed differences in spectral power, we computed a time–frequency spectrogram with a high resolution for pIPS (Fig. 6b). The lateralized change in gamma power extended into higher gamma frequencies above 64 Hz.

In a next step we investigated if the identified saccademetric specific signatures in pIPS differed between *guided* and *free* saccades (Fig. 6c). There was a significant difference in alpha power between hemifields contra- and ipsilateral to saccade direction for *free* as well as *guided* saccade trials during delay and saccade execution. This saccade direction specific effect was stronger for *guided* than *free* saccades during the delay period (t test, $p < 0.05$, FDR corrected for conditions, time, and frequency windows, $n = 3 \times 3 \times 2$). Only *guided* saccades showed significant stronger gamma power in contralateral versus ipsilateral sites of the pIPS in the delay period.

In summary, horizontal saccade direction was reflected in lateralized power changes in low gamma and alpha around the posterior parietal cortex. These lateralization effects were strongest during the delay period and stronger for *guided* trials.

Discussion

The goal of this study was to shed light on the spatiotemporal dynamics of action selection. To this end, we investigated the neuronal signatures of preparation, execution, and target selection for freely chosen and visually guided saccades. We found a fronto-parietal network exhibiting sustained power changes within gamma and alpha to beta frequency bands that may reflect the process of competition between behavioral alternatives for action selection.

In the first analysis combining *free* and *guided* saccades we identified significant changes of local oscillatory population activity related to general saccade planning and execution. In line with previous electrophysiological studies on sensorimotor transformations of guided saccades (Pesaran et al. 2002; Lachaux et al. 2006; Medendorp et al. 2007; Hinkley et al. 2011; Gregoriou et al. 2012), we identified a fronto-parietal network including the intraparietal sulcus and the frontal and supplementary eye fields, that exhibited an antagonistic signature of increased gamma band activity and suppressed beta band activity. Visual areas showed an additional increase in alpha band activity during the delay.

The neuronal activity we found for the combined analysis of *free* and *guided* saccades likely reflects different concurrently active processes including motor preparation,

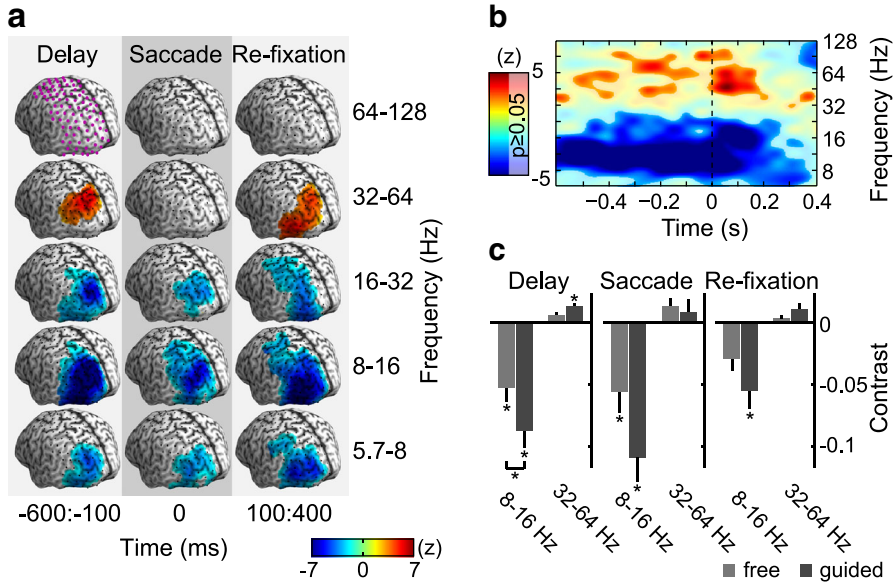

Fig. 6 Lateralized spectral signatures for horizontal saccades. **a** Differences in spectral power between contralateral and ipsilateral sites of saccade direction for horizontal saccades pooled over *free* and *guided* condition visualized onto a left cortical hemisphere. Cool color ranges denote less spectral power on contra—*relative* to ipsilateral sites of saccades direction, *warm colors* indicate stronger spectral power of contra—compared to ipsilateral sites. Statistical comparisons were restricted to 95 source locations in frontal, parietal and occipital areas (indicated by *purple dots* in the *upper left*). Difference from zero was statistically assessed by a cluster based random permutation test correcting for multiple comparisons of number of voxels, time windows, and frequency windows ($p < 0.05$). Functional maps are masked by the extent of the identified clusters and illustrated on a 3D cortical surface. **b** Time–frequency resolved differences in spectral power for contralateral versus ipsilateral parts of pIPS for horizontal saccades. The plot depicts statistically masked z-scores (*t* test, $p < 0.05$, uncorrected for multiple comparisons). **c** Differentiation of lateralization effects for *free* and *guided* saccades in selected frequency bands (alpha and low gamma) in pIPS. Lateralization is shown as the average contrast of spectral power of contra versus ipsilateral parts of pIPS (mean over subjects ± sem over subjects) for *free* (*light grey bars*) and *guided* (*dark grey bars*) saccades separately. Lateralization was tested against zero for both saccade types separately as well as for the difference between both conditions (*t* test, * $p < 0.05$, FDR corrected)

action selection, spatial attention, and working memory operations that need to be integrated for goal-oriented behavior. In order to unravel the mechanisms specific for action selection, we compared the neuronal activity for instructed action (*guided* saccades) with action selection between competing behavioral alternatives (*free* saccades). *Guided* saccade trials exhibited a stronger fast and transient gamma band response to the instructional cue compared to *free* saccade trials in extrastriate and posterior parietal cortex. In contrast, freely selecting saccade targets between equally valuable alternatives was associated with stronger subsequent sustained enhancements of fronto-parietal gamma power during the late preparation phase of the saccade.

Activity in the gamma frequency range is thought to reflect local excitatory-inhibitory interactions and can be regarded as a signature of enhanced cortical processing (Hasenstaub et al. 2005; Bartos et al. 2007; Cardin et al. 2009; Fries 2009; Donner and Siegel 2011). In this context, the fast transient and late persistent increases in gamma band in the contrast of *guided* and *free* saccades may reflect two distinct cortical processes associated with different aspects of action selection: Stronger gamma power for *guided* saccades directly after the cue may reflect fast orienting to the cued target location and action-relevant sensory response processes to the spatial cue. The protracted stronger increase of gamma band activity in free choice trials might reflect enhanced competition between various potential movement plans with equal rewarding outcomes compared to a single movement plan in *guided* saccades (cf. Cisek and Kalaska 2010). In particular, the sustained nature of the enhancement of gamma power in combination with its localization in areas of sensorimotor transformation is compatible with the assumption that the selection of actions emerges in a distributed way through mutual competition between cell assemblies that encode parallel evolving motor plans (Shadlen and Newsome 2001; Cisek and Kalaska 2005; Cui and Andersen 2007; Coulthard et al. 2008; Oliveira et al. 2010; Pastor-Bernier and Cisek 2011; Pastor-Bernier et al. 2012; Costello et al. 2013). Integrated models of action selection claim that this form of decision making is a general mechanism for all decisions resulting in a movement (Cisek 2006, 2007; Shadlen et al. 2008; Cisek and Kalaska 2010; cf. also Seth 2007).

How is this mutual competition between different action plans realized within the sensorimotor areas? Physiological measurements of single neuron activity in parietal cortex suggest that competition between multiple actions is encoded as relative rate code, reflecting the number of available options and the subjective desirability of each action alternative (Dorris and Glimcher 2004; Sugrue et al. 2004; Klaes et al. 2012). On the population level, we observed a global enhancement of gamma power in fronto-parietal association cortex associated with the presence of multiple action alternatives. The observed gamma band signature is distinct from saccadic spike artifact activity with respect to source localization and to temporal dynamics and therefore most likely arises from neuronal rhythmic synchronization (cf. Jerbi et al. 2009 and Carl et al. 2012 for source distribution of the saccadic spike artifact in iEEG and MEG, respectively). This enhancement of local rhythmic inhibitory-excitatory interactions may reflect enhanced local competition between cell assemblies. Hence, our observations suggest that in addition to spike rates, precise timing—reflected in synchronization—plays a role in the competition between cell assemblies representing different available action alternatives.

Because all choices in the *free* saccade trials were behaviorally equally valuable in our experiment, subjects were free to choose and had to motivate their choice internally. Interpreting this as a form of voluntary choice, our findings corroborate studies that have attributed aspects of voluntariness of action selection to the fronto-parietal network. Human fMRI, TMS, and lesion studies suggested that parietal and premotor areas are involved in the process of voluntary or free action selection (Milea et al. 2007; Soon et al. 2008; Beudel and de Jong 2009; Oliveira et al. 2010). Furthermore, the fronto-parietal network was proposed to specifically implement the choice of an action when maximally competing alternatives are present (Haggard 2008; Kable and Glimcher 2009; de Jong 2011). This assumption is supported by electrophysiological studies in non-human primates that found single unit activity in lateral intraparietal area and oscillatory coupling between premotor and parietal areas representing the specific outcome of a chosen movement amongst competing alternatives (Gold and Shadlen 2007; Pesaran et al. 2008). Our findings of enhanced fronto-parietal gamma activity during saccade target selection provides evidence for a similar choice network in humans and suggests an important role of oscillatory activity for implementing voluntary action selection.

Various cerebral structures have been associated with the origin of voluntary decisions. While e.g. Soon et al. (2008) and Bode et al. (2012) suggested that frontopolar cortex implements the initial step in generating decisions, other evidence points to medial frontal cortex as a key player in intentional action selection in humans (Libet et al. 1983; Cunnington et al. 2002; Rowe et al. 2010; Fried et al. 2011). Our data do not exclude the possibility that structures like medial frontal cortex including the supplementary eye fields might modulate other fronto-parietal structures in order to mediate saccade target selection (cf. Coe et al. 2002). Here, our data showing concurrent sustained fronto-parietal oscillatory activity associated with free action selection support assumptions about decisions being implemented in a network of concurrently active brain areas operating in a parallel manner (Ledberg et al. 2007).

An important question is to what degree attentional mechanisms might contribute to the selection specific differences in gamma power between *free* and *guided* saccades. Since spatial orienting implicates spatial attention, choosing spatial saccade targets is correlated to some degree with attentional shifts (cf. Andersen and Cui 2009), and there is good evidence that overt orienting and covert attention are mediated partly by the same networks (Rizzolatti et al. 1987; Kustov and Robinson 1996; Corbetta et al. 1998). We understand decision towards action as an emergent phenomenon that is necessarily composed of several sub-functions including attentional contributions. In line with this argument Bisley and Goldberg (2010), proposed the concept of priority maps that highlight behaviorally relevant information to bias sensorimotor systems for appropriate action selections with the lateral intraparietal area as a neural substrate. Our data support the hypothesis of a similar priority map in humans.

Similarly, memory processes for strategic considerations might accompany voluntary saccade target selection. An inhibition of choosing the preceding target in most subjects suggests that observed selection specific power signatures might to some extent be related to monitoring of response history (cf. Rowe et al. 2010; Zhang et al. 2012). Such an action monitoring may be part of an integrated process of motor planning, action selection, attentional allocation, and working memory (Cisek and Kalaska 2005; Jerde et al. 2012).

Finally, the stronger transient response to *guided* compared to *free* saccades may relate to processes other than action selection: First, sensory responses may differ between conditions due to physical differences between cue colors. However, isoluminant changes in visual stimuli, as employed here, have been shown to induce only weak gamma band responses confined to early visual areas (Swettenham et al. 2013; cf. also Adjamian et al. 2008), making a purely sensory driven difference of high gamma band power between conditions in parietal and extrastriate areas unlikely. In addition, evidence from non-human primates suggests that the strength of sensory responses

within parietal areas relies on behavioral relevance of the stimulus (cf. Toth and Assad 2002; Ipata et al. 2006; Andersen and Cui 2009) and hence is not independent from processes related to spatial guidance to the saccade target. Second, *guided* saccades where the target must be kept in memory after cue offset may entail higher working memory load than *free* saccades. Although spectral and spatial distributions for the stronger cue-related power increase in *guided* saccades are compatible with such a view, the transient nature of the observed effect renders this interpretation implausible (Curtis and Lee 2010).

In addition to the selection specific changes in gamma power, we found that power was reduced within alpha and beta bands during *free* saccade target selection compared to *guided* saccades. These lower frequency changes spatially overlapped with the changes in the gamma band but were more widespread. Spectrally, these effects are compatible with the rolandic mu rhythm with the alpha band reflecting predominantly somatosensory cortical function and the beta band reflecting motor-cortex function (Hari and Salmelin 1997).

Beta band activity has been related to maintaining the status quo of sensorimotor or cognitive states (Engel and Fries 2010). Its suppression has been associated with activation of sensorimotor areas during voluntary movement preparation and execution, motor imagery and movement observation for limb movements (Hari et al. 1998; Neuper and Pfurtscheller 1999, Pfurtscheller and Lopes da Silva 1999) and may reflect a general readiness for change. In particular, beta band suppression was shown to be enhanced in motor cortex when competing motor plans are co-activated in a manual Erikson flanker paradigm (Grent-'t-Jong et al. 2013) and beta band suppression seems to reflect the formation of a decision as a preparatory motor signal based on the integrated evidence in perceptual decisions (Donner et al. 2009; Wyart et al. 2012). Oscillations in the alpha band have been implicated in a gating mechanism that inhibits task irrelevant areas or, by release of inhibition, enhances the general excitability of task relevant areas (Klimesch et al. 2007; Jensen and Mazaheri 2010). Such a gating function is known to be associated with allocation of spatial attention (Thut et al. 2006; Siegel et al. 2008; Wyart and Tallon-Baudry 2008). Consequently, the observed effects of less spectral power in alpha and beta frequency ranges during *free* action selection compared to *guided* saccade trials may reflect stronger engagement in movement preparation for multiple actions plans as well as differences in attentional load, or a combination of both effects.

To further pinpoint the functional role of the spectral signatures of saccade target selection we investigated their directional specificity. In line with previous reports on *guided* saccades (Medendorp et al. 2007; Van Der Werf et al. 2008; 2010; Buchholz et al. 2011; Van Der Werf et al. 2013), we found lateralized gamma band activity in pIPS and lateralized alpha modulations in posterior parietal and extrastriate areas. However, directional specificity in pIPS was much less pronounced for *free* compared to *guided* saccades. A possible explanation is that lateralization effects gradually build up with the evolvement of a decision for the *free* saccade trials, resulting in overall weaker spectral lateralization. Further studies are needed to elaborate on the direction specific dynamics of the selection process in presentence of competing alternatives.

To conclude, our data show that action selection for instructed behavior dissociates from internally motivated action selection between behavioral alternatives in spectral signatures, with stronger fast transient gamma band responses for instructed and later sustained gamma band activity for freely selected saccades in a fronto-parietal network. These spectro-temporal characteristics may reflect an integrated and parallelized process of eye movement selection when selection between competing movements is required.

Acknowledgments This study was supported by grants from the European Union (EU) (IST-2005-27268, FP7-ICT-270212, ERC-2010-AdG-269716) and the Deutsche Forschungsgemeinschaft (DFG) (SFB 936/A3/B6).

Conflict of interest The authors declare no competing financial interests.

Ethical Standards The Ethics Committee of the Medical Association Hamburg approved the current study. The study was conducted in accordance with the Declaration of Helsinki and informed consent was obtained from all participants prior to recordings. The manuscript does not contain clinical studies or patient data.

References

Adjamian P, Hadjipapas A, Barnes GR, Hillebrand A, Holliday IE (2008) Induced gamma activity in primary visual cortex is related to luminance and not color contrast: an MEG study. J Vis 8(4):1–7. doi:10.1167/8.7.4

Andersen RA, Cui H (2009) Intention, action planning, and decision making in parietal-frontal circuits. Neuron 63:568–583. doi:10.1016/j.neuron.2009.08.028

Anderson EJ, Jones DK, O'Gorman RL et al (2012) Cortical network for gaze control in humans revealed using multimodal MRI. Cereb Cortex 22:765–775. doi:10.1093/cercor/bhr110

Bartos M, Vida I, Jonas P (2007) Synaptic mechanisms of synchronized gamma oscillations in inhibitory interneuron networks. Nat Rev Neurosci 8:45–56. doi:10.1038/nrn2044

Benjamini Y, Hochberg Y (1995) Controlling the false discovery rate: a practical and powerful approach to multiple testing. J R Statistic Soc Series B (Methodological) 57:289–300

Beudel M, de Jong BM (2009) Overlap and segregation in predorsal premotor cortex activations related to free selection of self-referenced and target-based finger movements. Cereb Cortex 19:2361–2371. doi:10.1093/cercor/bhn254

Bisley JW, Goldberg ME (2010) Attention, intention, and priority in the parietal lobe. Annu Rev Neurosci 33:1–21. doi:10.1146/annurev-neuro-060909-152823

Bode S, Bogler C, Soon CS, Haynes J-D (2012) The neural encoding of guesses in the human brain. Neuroimage 59:1924–1931. doi:10.1016/j.neuroimage.2011.08.106

Buchholz VN, Jensen O, Medendorp WP (2011) Multiple reference frames in cortical oscillatory activity during tactile remapping for saccades. J Neurosci 31:16864–16871. doi:10.1523/jneurosci.3404-11.2011

Cardin JA, Carlén M, Meletis K, Knoblich U, Zhang F, Deisseroth K, Tsai L-H, Moore CI (2009) Driving fast-spiking cells induces gamma rhythm and controls sensory responses. Nature 459:663–667. doi:10.1038/nature08002

Carl C, Açık A, König P, Engel AK, Hipp JF (2012) The saccadic spike artifact in MEG. Neuroimage 59:1657–1667. doi:10.1016/j.neuroimage.2011.09.020

Cisek P (2006) Integrated neural processes for defining potential actions and deciding between them: a computational model. J Neurosci 26:9761–9770. doi:10.1523/jneurosci.5605-05.2006

Cisek P (2007) Cortical mechanisms of action selection: the affordance competition hypothesis. Philos Trans R Soc Lond B Biol Sci 362:1585–1599. doi:10.1098/rstb.2007.2054

Cisek P (2012) Making decisions through a distributed consensus. Curr Opin Neurobiol 22:927–936. doi:10.1016/j.conb.2012.05.007

Cisek P, Kalaska JF (2005) Neural correlates of reaching decisions in dorsal premotor cortex: specification of multiple direction choices and final selection of action. Neuron 45:801–814. doi:10.1016/j.neuron.2005.01.027

Cisek P, Kalaska JF (2010) Neural mechanisms for interacting with a world full of action choices. Annu Rev Neurosci 33:269–298. doi:10.1146/annurev.neuro.051508.135409

Coe B, Tomihara K, Matsuzawa M, Hikosaka O (2002) Visual and anticipatory bias in three cortical eye fields of the monkey during an adaptive decision-making task. J Neurosci 22:5081–5090

Corbetta M, Akbudak E, Conturo TE, Snyder AZ, Ollinger JM, Drury HA, Linenweber MR, Petersen SE, Raichle ME, Van Essen DC, Shulman GL (1998) A common network of functional areas for attention and eye movements. Neuron 21:761–773

Costello MG, Zhu D, Salinas E, Stanford TR (2013) Perceptual modulation of motor–but not visual–responses in the frontal eye field during an urgent-decision task. J Neurosci 33:16394–16408. doi:10.1523/jneurosci.1899-13.2013

Coulthard EJ, Nachev P, Husain M (2008) Control over conflict during movement preparation: role of posterior parietal cortex. Neuron 58:144–157. doi:10.1016/j.neuron.2008.02.009

Croft RJ, Barry RJ (2000) Removal of ocular artifact from the EEG: a review. Neurophysiol Clin 30:5–19. doi:10.1016/S0987-7053(00)00055-1

Cui H, Andersen RA (2007) Posterior parietal cortex encodes autonomously selected motor plans. Neuron 56:552–559. doi:10.1016/j.neuron.2007.09.031

Cunnington R, Windischberger C, Deecke L, Moser E (2002) The preparation and execution of self-initiated and externally-triggered movement: a study of event-related fMRI. Neuroimage 15:373–385. doi:10.1006/nimg.2001.0976

Curtis CE, Lee D (2010) Beyond working memory: the role of persistent activity in decision making. Trends Cogn Sci 14:216–222. doi:10.1016/j.tics.2010.03.006

de Jong BM (2011) Neurology of widely embedded free will. Cortex 47:1160–1165. doi:10.1016/j.cortex.2011.06.011

Donner TH, Siegel M (2011) A framework for local cortical oscillation patterns. Trends Cogn Sci 15:191–199. doi:10.1016/j.tics.2011.03.007

Donner TH, Siegel M, Fries P, Engel AK (2009) Buildup of choice-predictive activity in human motor cortex during perceptual decision making. Curr Biol 19:1581–1585. doi:10.1016/j.cub.2009.07.066

Dorris MC, Glimcher PW (2004) Activity in posterior parietal cortex is correlated with the relative subjective desirability of action. Neuron 44:365–378. doi:10.1016/j.neuron.2004.09.009

Engel AK, Fries P (2010) Beta-band oscillations—signalling the status quo? Curr Opin Neurobiol 20:156–165. doi:10.1016/j.conb.2010.02.015

Engel AK, Maye A, Kurthen M, König P (2013) Where's the action? The pragmatic turn in cognitive science. Trends Cogn Sci 17:202–209. doi:10.1016/j.tics.2013.03.006

Fried I, Mukamel R, Kreiman G (2011) Internally generated preactivation of single neurons in human medial frontal cortex predicts volition. Neuron 69:548–562. doi:10.1016/j.neuron.2010.11.045

Fries P (2009) Neuronal gamma-band synchronization as a fundamental process in cortical computation. Annu Rev Neurosci 32:209–224. doi:10.1146/annurev.neuro.051508.135603

Genovese CR, Lazar NA, Nichols T (2002) Thresholding of statistical maps in functional neuroimaging using the false discovery rate. Neuroimage 15:870–878. doi:10.1006/nimg.2001.1037

Glimcher PW (2003) The neurobiology of visual-saccadic decision making. Annu Rev Neurosci 26:133–179. doi:10.1146/annurev.neuro.26.010302.081134

Gold JI, Shadlen MN (2007) The neural basis of decision making. Annu Rev Neurosci 30:535–574. doi:10.1146/annurev.neuro.29.051605.113038

Gould IC, Nobre AC, Wyart V, Rushworth MFS (2012) Effects of decision variables and intraparietal stimulation on sensorimotor oscillatory activity in the human brain. J Neurosci 32:13805–13818. doi:10.1523/jneurosci.2200-12.2012

Gratton G, Coles MG, Donchin E (1983) A new method for off-line removal of ocular artifact. Electroencephalogr Clin Neurophysiol 55:468–484

Gregoriou GG, Gotts SJ, Desimone R (2012) Cell-type-specific synchronization of neural activity in FEF with V4 during attention. Neuron 73:581–594. doi:10.1016/j.neuron.2011.12.019

Grent-'t-Jong T, Oostenveld R, Jensen O et al (2013) Oscillatory dynamics of response competition in human sensorimotor cortex. Neuroimage 83:27–34. doi:10.1016/j.neuroimage.2013.06.051

Gross J, Kujala J, Hämäläinen M, Timmermann L, Schnitzler A, Salmelin R (2001) Dynamic imaging of coherent sources: studying neural interactions in the human brain. Proc Natl Acad Sci USA 98:694–699. doi:10.1073/pnas.98.2.694

Haggard P (2008) Human volition: towards a neuroscience of will. Nat Rev Neurosci 9:934–946. doi:10.1038/nrn2497

Hare TA, Schultz W, Camerer CF, O'Doherty JP, Rangel A (2011) Transformation of stimulus value signals into motor commands during simple choice. Proc Natl Acad Sci USA 108:18120–18125. doi:10.1073/pnas.1109322108

Hari R, Salmelin R (1997) Human cortical oscillations: a neuromagnetic view through the skull. Trends Neurosci 20:44–49. doi:10.1016/S0166-2236(96)10065-5

Hari R, Forss N, Avikainen S et al (1998) Activation of human primary motor cortex during action observation: a neuromagnetic study. Proc Natl Acad Sci USA 95:15061–15065

Hasenstaub A, Shu Y, Haider B, Kraushaar U, Duque A, McCormick DA (2005) Inhibitory postsynaptic potentials carry synchronized frequency information in active cortical networks. Neuron 47:423–435. doi:10.1016/j.neuron.2005.06.016

Hassler U, Barreto NT, Gruber T (2011) Induced gamma band responses in human EEG after the control of miniature saccadic artifacts. Neuroimage 57:1411–1421. doi:10.1016/j.neuroimage.2011.05.062

Hinkley LBN, Nagarajan SS, Dalal SS, Guggisberg AG, Disbrow EA (2011) Cortical temporal dynamics of visually guided behavior. Cereb Cortex 21:519–529. doi:10.1093/cercor/bhq102

Hipp JF, Siegel M (2013) Dissociating neuronal gamma-band activity from cranial and ocular muscle activity in EEG. Front Hum Neurosci 7:338. doi:10.3389/fnhum.2013.00338

Hipp JF, Engel AK, Siegel M (2011) Oscillatory synchronization in large-scale cortical networks predicts perception. Neuron 69:387–396. doi:10.1016/j.neuron.2010.12.027

Holmes CJ, Hoge R, Collins L, Woods R, Toga AW, Evans AC (1998) Enhancement of MR images using registration for signal averaging. J Comput Assist Tomogr 22:324–333

Hoshi E, Tanji J (2007) Distinctions between dorsal and ventral premotor areas: anatomical connectivity and functional properties. Curr Opin Neurobiol 17:234–242. doi:10.1016/j.conb.2007.02.003

Hyvärinen A, Oja E (2000) Independent component analysis: algorithms and applications. Neural Netw 13:411–430

Ipata AE, Gee AL, Gottlieb J, Bisley JW, Goldberg ME (2006) LIP responses to a popout stimulus are reduced if it is overtly ignored. Nat Neurosci 9:1071–1076. doi:10.1038/nn1734

Jensen O, Mazaheri A (2010) Shaping functional architecture by oscillatory alpha activity: gating by inhibition. Front Hum Neurosci 4:186. doi:10.3389/fnhum.2010.00186

Jerbi K, Freyermuth S, Dalal S, Kahane P, Bertrand O, Berthoz A, Lachaux J-P (2009) Saccade related gamma-band activity in intracerebral EEG: dissociating neural from ocular muscle activity. Brain Topogr 22:18–23. doi:10.1007/s10548-009-0078-5

Jerde TA, Merriam EP, Riggall AC, Hedges JH, Curtis CE (2012) Prioritized maps of space in human frontoparietal cortex. J Neurosci 32:17382–17390. doi:10.1523/jneurosci.3810-12.2012

Jung TP, Makeig S, Westerfield M et al (2000) Removal of eye activity artifacts from visual event-related potentials in normal and clinical subjects. Neurophysiol Clin 111:1745–1758

Kable JW, Glimcher PW (2009) The neurobiology of decision: consensus and controversy. Neuron 63:733–745. doi:10.1016/j.neuron.2009.09.003

Kagan I, Iyer A, Lindner A, Andersen RA (2010) Space representation for eye movements is more contralateral in monkeys than in humans. Proc Natl Acad Sci USA 107:7933–7938. doi:10.1073/pnas.1002825107

Keren AS, Yuval-Greenberg S, Deouell LY (2010) Saccadic spike potentials in gamma-band EEG: characterization, detection and suppression. Neuroimage 49:2248–2263. doi:10.1016/j.neuroimage.2009.10.057

Klaes C, Schneegans S, Schöner G, Gail A (2012) Sensorimotor learning biases choice behavior: a learning neural field model for decision making. PLoS Comp Biol 8:e1002774. doi:10.1371/journal.pcbi.1002774

Klimesch W, Sauseng P, Hanslmayr S (2007) EEG alpha oscillations: the inhibition-timing hypothesis. Brain Res Rev 53:63–88. doi:10.1016/j.brainresrev.2006.06.003

Kovach CK, Tsuchiya N, Kawasaki H, Oya H, Howard MA, Adolphs R (2011) Manifestation of ocular-muscle EMG contamination in human intracranial recordings. Neuroimage 54:213–233. doi:10.1016/j.neuroimage.2010.08.002

Kustov AA, Robinson DL (1996) Shared neural control of attentional shifts and eye movements. Nature 384:74–77. doi:10.1038/384074a0

Lachaux J-P, Hoffmann D, Minotti L, Berthoz A, Kahane P (2006) Intracerebral dynamics of saccade generation in the human frontal eye field and supplementary eye field. Neuroimage 30:1302–1312. doi:10.1016/j.neuroimage.2005.11.023

Lancaster JL, Tordesillas-Gutiérrez D, Martinez M, Salinas F, Evans A, Zilles K, Mazziotta JC, Fox PT (2007) Bias between MNI and Talairach coordinates analyzed using the ICBM-152 brain template. Hum Brain Mapp 28:1194–1205. doi:10.1002/hbm.20345

Lawrence BM, Snyder LH (2006) Comparison of effector-specific signals in frontal and parietal cortices. J Neurophysiol 96:1393–1400. doi:10.1152/jn.01368.2005

Ledberg A, Bressler SL, Ding M, Coppola R, Nakamura R (2007) Large-scale visuomotor integration in the cerebral cortex. Cereb Cortex 17:44–62. doi:10.1093/cercor/bhj123

Lee TW, Girolami M, Sejnowski TJ (1999) Independent component analysis using an extended infomax algorithm for mixed subgaussian and supergaussian sources. Neural Comput 11:417–441

Libet B, Gleason CA, Wright EW, Pearl DK (1983) Time of conscious intention to act in relation to onset of cerebral activity (readiness-potential). The unconscious initiation of a freely voluntary act. Brain 106:623–642

McDowell JE, Dyckman KA, Austin BP, Clementz BA (2008) Neurophysiology and neuroanatomy of reflexive and volitional saccades: evidence from studies of humans. Brain Cogn 68:255–270. doi:10.1016/j.bandc.2008.08.016

Medendorp WP, Kramer GFI, Jensen O, Oostenveld R, Schoffelen J-M, Fries P (2007) Oscillatory activity in human parietal and occipital cortex shows hemispheric lateralization and memory effects in a delayed double-step saccade task. Cereb Cortex 17:2364–2374. doi:10.1093/cercor/bhl145

Medendorp WP, Buchholz VN, Van Der Werf J, Leoné FTM (2011) Parietofrontal circuits in goal-oriented behaviour. Eur J Neurosci 33:2017–2027. doi:10.1111/j.1460-9568.2011.07701.x

Milea D, Lobel E, Lehéricy S, Leboucher P, Pochon J-B, Pierrot-Deseilligny C, Berthoz A (2007) Prefrontal cortex is involved in internal decision of forthcoming saccades. NeuroReport 18:1221–1224. doi:10.1097/WNR.0b013e3281e72ce7

Mitra PP, Pesaran B (1999) Analysis of dynamic brain imaging data. Biophys J 76:691–708. doi:10.1016/S0006-3495(99)77236-X

Neuper C, Pfurtscheller G (1999) Motor imagery and ERD. In: Pfurtscheller G, Lopes da Silva FH (eds) Event-related desynchronization. Handbook of electroencephalography and clinical neurophysiology, vol 6. Elsevier, Amsterdam, pp 303–325

Nichols TE, Holmes AP (2002) Nonparametric permutation tests for functional neuroimaging: a primer with examples. Hum Brain Mapp 15:1–25

Nolte G (2003) The magnetic lead field theorem in the quasi-static approximation and its use for magnetoencephalography forward calculation in realistic volume conductors. Phys Med Biol 48:3637–3652. doi:10.1088/0031-9155/48/22/002

Oliveira FTP, Diedrichsen J, Verstynen T, Duque J, Ivry RB (2010) Transcranial magnetic stimulation of posterior parietal cortex affects decisions of hand choice. Proc Natl Acad Sci USA 107:17751–17756. doi:10.1073/pnas.1006223107

Oostenveld R, Fries P, Maris E, Schoffelen J-M (2011) FieldTrip: open source software for advanced analysis of MEG, EEG, and invasive electrophysiological data. Comput Intell Neurosci 2011:156869. doi:10.1155/2011/156869

Pastor-Bernier A, Cisek P (2011) Neural correlates of biased competition in premotor cortex. J Neurosci 31:7083–7088. doi:10.1523/jneurosci.5681-10.2011

Pastor-Bernier A, Tremblay E, Cisek P (2012) Dorsal premotor cortex is involved in switching motor plans. Front Neuroeng 5(5):1–15. doi:10.3389/fneng.2012.00005

Pesaran B, Pezaris JS, Sahani M, Mitra PP, Andersen RA (2002) Temporal structure in neuronal activity during working memory in macaque parietal cortex. Nat Neurosci 5:805–811. doi:10.1038/nn890

Pesaran B, Nelson MJ, Andersen RA (2008) Free choice activates a decision circuit between frontal and parietal cortex. Nature 453:406–409. doi:10.1038/nature06849

Pfurtscheller G, Lopes da Silva FH (1999) Event-related EEG/MEG synchronization and desynchronization: basic principles.

Neurophysiol Clin 110:1842–1857. doi:10.1016/S1388-2457(99)00141-8

Plöchl M, Ossandón JP, König P (2012) Combining EEG and eye tracking: identification, characterization, and correction of eye movement artifacts in electroencephalographic data. Front Hum Neurosci 6:278. doi:10.3389/fnhum.2012.00278

R Core Team (2013) R: a language and environment for statistical computing (R foundation for statistical computing, ed). Vienna

Rizzolatti G, Riggio L, Dascola I, Umiltá C (1987) Reorienting attention across the horizontal and vertical meridians: evidence in favor of a premotor theory of attention. Neuropsychologia 25:31–40

Rowe JB, Hughes L, Nimmo-Smith I (2010) Action selection: a race model for selected and non-selected actions distinguishes the contribution of premotor and prefrontal areas. Neuroimage 51:888–896. doi:10.1016/j.neuroimage.2010.02.045

Salvucci DD, Goldberg JH (2000) Identifying fixations and saccades in eye-tracking protocols. Proceedings of the symposium on eye tracking research & applications—ETRA '00 (Florida). ACM Press, New York, pp 71–78

Schlögl A, Keinrath C, Zimmermann D, Scherer R, Leeb R, Pfurtscheller G (2007) A fully automated correction method of EOG artifacts in EEG recordings. Neurophysiol Clin 118:98–104. doi:10.1016/j.clinph.2006.09.003

Seth AK (2007) The ecology of action selection: insights from artificial life. Philos Trans R Soc Lond B Biol Sci 362(1485):1545–1558. doi:10.1098/rstb.2007.2052

Shadlen MN, Newsome WT (2001) Neural basis of a perceptual decision in the parietal cortex (area LIP) of the rhesus monkey. J Neurophysiol 86:1916–1936

Shadlen MN, Kiani R, Hanks TD, Churchland AK (2008) Neurobiology of decision making: An intentional framework. In: Engel C, Singer W (eds) Better than conscious? Decision making, the human mind, and implications for institutions. MIT Press, Cambridge, pp 71–101

Siegel M, Donner TH, Oostenveld R, Fries P, Engel AK (2008) Neuronal synchronization along the dorsal visual pathway reflects the focus of spatial attention. Neuron 60:709–719. doi:10.1016/j.neuron.2008.09.010

Siegel M, Engel AK, Donner TH (2011) Cortical network dynamics of perceptual decision-making in the human brain. Front Hum Neurosci 5(21):1–12. doi:10.3389/fnhum.2011.00021

Soon CS, Brass M, Heinze H-J, Haynes J-D (2008) Unconscious determinants of free decisions in the human brain. Nat Neurosci 11:543–545. doi:10.1038/nn.2112

Sugrue LP, Corrado GS, Newsome WT (2004) Matching behavior and the representation of value in the parietal cortex. Science 304:1782–1787. doi:10.1126/science.1094765

Sweeney JA, Luna B, Keedy SK et al (2007) fMRI studies of eye movement control: investigating the interaction of cognitive and sensorimotor brain systems. Neuroimage 36(Suppl 2):T54–T60. doi:10.1016/j.neuroimage.2007.03.018

Swettenham JB, Muthukumaraswamy SD, Singh KD (2013) BOLD responses in human primary visual cortex are insensitive to substantial changes in neural activity. Front Hum Neurosci. doi:10.3389/fnhum.2013.00076

Thomson DJ (1982) Spectrum estimation and harmonic analysis. Proc IEEE 70:1055–1096. doi:10.1109/proc.1982.12433

Thut G, Nietzel A, Brandt SA, Pascual-Leone A (2006) Alpha-band electroencephalographic activity over occipital cortex indexes visuospatial attention bias and predicts visual target detection. J Neurosci 26:9494–9502. doi:10.1523/jneurosci.0875-06.2006

Toth LJ, Assad JA (2002) Dynamic coding of behaviourally relevant stimuli in parietal cortex. Nature 415:165–168. doi:10.1038/415165a

Van Der Werf J, Jensen O, Fries P, Medendorp WP (2008) Gamma-band activity in human posterior parietal cortex encodes the motor goal during delayed prosaccades and antisaccades. J Neurosci 28:8397–8405. doi:10.1523/jneurosci.0630-08.2008

Van Der Werf J, Jensen O, Fries P, Medendorp WP (2010) Neuronal synchronization in human posterior parietal cortex during reach planning. J Neurosci 30:1402–1412. doi:10.1523/jneurosci.3448-09.2010

Van Der Werf J, Buchholz VN, Jensen O, Medendorp WP (2013) Reorganization of oscillatory activity in human parietal cortex during spatial updating. Cereb Cortex 23:508–519. doi:10.1093/cercor/bhr387

Van Veen BD, Van Drongelen W, Yuchtman M, Suzuki A (1997) Localization of brain electrical activity via linearly constrained minimum variance spatial filtering. IEEE Trans Biomed Eng 44:867–880. doi:10.1109/10.623056

Wyart V, Tallon-Baudry C (2008) Neural dissociation between visual awareness and spatial attention. J Neurosci 28:2667–2679. doi:10.1523/jneurosci.4748-07.2008

Wyart V, de Gardelle V, Scholl J, Summerfield C (2012) Rhythmic fluctuations in evidence accumulation during decision making in the human brain. Neuron 76:847–858. doi:10.1016/j.neuron.2012.09.015

Yuval-Greenberg S, Tomer O, Keren AS, Nelken I, Deouell LY (2008) Transient induced gamma-band response in EEG as a manifestation of miniature saccades. Neuron 58:429–441. doi:10.1016/j.neuron.2008.03.027

Zhang J, Hughes LE, Rowe JB (2012) Selection and inhibition mechanisms for human voluntary action decisions. Neuroimage 63:392–402. doi:10.1016/j.neuron.2011.10.035